The Journal of Experimental Biology 202, 2139–2150 (1999)
Printed in Great Britain © The Company of Biologists Limited 1999
JEB2125

MUSCLE DYNAMICS IN SKIPJACK TUNA: TIMING OF RED MUSCLE SHORTENING IN RELATION TO ACTIVATION AND BODY CURVATURE DURING STEADY SWIMMING

ROBERT E. SHADWICK[1,*], STEPHEN L. KATZ[1,‡], KEITH E. KORSMEYER[1,§], TORRE KNOWER[1] AND JAMES W. COVELL[2]

[1]*Marine Biology Research Division, Scripps Institution of Oceanography, La Jolla, CA 92093-0204, USA* and [2]*Department of Medicine, University of California, San Diego, La Jolla, CA 92093-0613, USA*

*e-mail: rshadwick@ucsd.edu

‡Present address: Department of Zoology, Duke University, Durham, NC 27708-0325, USA

§Present address: Hawaii Pacific University, 45-045 Kamehameha Highway, Kaneohe, HI 96744-5297, USA

Accepted 25 April; published on WWW 19 July 1999

Summary

Cyclic length changes in the internal red muscle of skipjack tuna (*Katsuwonus pelamis*) were measured using sonomicrometry while the fish swam in a water tunnel at steady speeds of 1.1–2.3 $L\,s^{-1}$, where L is fork length. These data were coupled with simultaneous electromyographic (EMG) recordings. The onset of EMG activity occurred at virtually the same phase of the strain cycle for muscle at axial locations between approximately 0.4L and 0.74L, where the majority of the internal red muscle is located. Furthermore, EMG activity always began during muscle lengthening, 40–50 ° prior to peak length, suggesting that force enhancement by stretching and net positive work probably occur in red muscle all along the body. Our results support the idea that positive contractile power is derived from all the aerobic swimming muscle in tunas, while force transmission is provided primarily by connective tissue structures, such as skin and tendons, rather than by muscles performing negative work.

We also compared measured muscle length changes with midline curvature (as a potential index of muscle strain) calculated from synchronised video image analysis. Unlike contraction of the superficial red muscle in other fish, the shortening of internal red muscle in skipjack tuna substantially lags behind changes in the local midline curvature. The temporal separation of red muscle shortening and local curvature is so pronounced that, in the mid-body region, muscle shortening at each location is synchronous with midline curvature at locations that are 7–8 cm (i.e. 8–10 vertebral segments) more posterior. These results suggest that contraction of the internal red muscle causes deformation of the body at more posterior locations, rather than locally. This situation represents a unique departure from the model of a homogeneous bending beam, which describes red muscle strain in other fish during steady swimming, but is consistent with the idea that tunas produce thrust by motion of the caudal fin rather than by undulation of segments along the body.

Key words: muscle activation, muscle strain, electromyography, tuna, *Katsuwonus pelamis*, swimming, red muscle, sonomicrometry.

Introduction

The axial muscle that powers undulatory swimming in fishes is complex in structure as well as dynamic function. The myotomal muscle of most fish consists of a series of folded and nested cones, one attaching to the next as well as to the adjacent skin and axial skeleton by various connective tissue linkages. Activation of the muscle is by a progression of electrical activity that travels posteriorly and alternately along each side of the body. These events result in coordinated, sequential contractions that are manifest as a wave of lateral deformation that grows in amplitude as it progresses along the body. An additional feature in fish is the anatomical distinction between oxidative red muscle, used for steady swimming and typically found in a thin subdermal band, and the glycolytic white muscle, used for high-speed bursting and making up the bulk of the myotome cones (Bone, 1978).

Among teleosts, tunas have remarkable anatomical specialisations that are usually associated with high-performance locomotion (Fierstine and Walters, 1968; Magnuson, 1978; Brill, 1996). In addition to the stream-lined, bullet-shaped body and high-aspect-ratio hydrofoil-like caudal fin, two other features are of particular importance to our study of muscle function: the myotomes are highly elongate and have tendinous attachments to the axial skeleton, and the red muscle is located primarily within the nested myotomal cones (Kishinouye, 1923; Graham et al., 1983; see Fig. 2B). It is clear that this red muscle powers steady swimming (Rayner

and Keenan, 1967; Brill and Dizon, 1979; Knower et al., 1999), but nothing is known about its contractile performance *in vivo* or of the mechanical consequences of its internal placement. Hence, the objective of the present study was to measure the kinematic properties of the internal red muscle in swimming skipjack tuna *Katsuwonus pelamis.*

Timing of muscle activation in vivo

Many studies of fish swimming mechanics and energetics have focused on the temporal relationship between the activation of muscle and its strain cycle *in vivo* (for a review, see Shadwick et al., 1998). Apparent differences in the rates at which the waves of muscle activation and body bending travel posteriorly have led to the suggestion, in many cases, that anteriorly and posteriorly located muscle must operate under different combinations of strain and stimulation, and thus have different functions in swimming (Williams et al., 1989; van Leeuwen et al., 1990; Altringham et al., 1993; Rome et al., 1993; Videler, 1993; Wardle and Videler, 1993; Wardle et al., 1995; Coughlin and Rome, 1996; Long, 1998). *In vitro* work-loop studies that mimic the range of observed patterns of contraction have shown that the contractile work done, and consequently the power produced by fish muscle, is highly dependent on, among other things, the timing of the electrical activation relative to the phase of the strain cycle (Altringham and Johnston, 1990; Johnson and Johnston, 1991; Rome et al., 1993). For example, if a muscle is activated just prior to peak length, it can develop and maintain large forces during shortening and relax fully during lengthening, thereby performing largely positive work. In contrast, a muscle that is activated only while lengthening may perform net negative work, i.e. the work done on the muscle to extend it will exceed the contractile work produced during shortening. Clearly, the prediction of muscle function in a swimming fish depends on the accurate determination of the timing of electromyographic (EMG) activity and muscle strain *in vivo*. Muscle strain during swimming can be calculated from the local curvature of the body midline or measured directly using a technique such as sonomicrometry. These methods have been shown to be equivalent in spite of the complex myotome anatomy found in fish. For example, studies in which muscle strain, calculated from midline kinematics, was compared with direct measurements of *in vivo* muscle length changes, made using sonomicrometry (Coughlin et al., 1996; Katz et al., 1999) or using videoradiography (Shadwick et al., 1998), have confirmed that the strain cycle in superficial red muscle in scup (*Stenotomus chrysops*), milkfish (*Chanos chanos*) and mackerel (*Scomber japonicus*) is highly correlated with changes in local curvature. Therefore, a simple beam is an appropriate model for calculating the magnitude and phase of strain in red muscle during steady swimming of those fish and probably others (e.g. Hess and Videler, 1984; van Leeuwen et al., 1990; Jayne and Lauder, 1995; Cheng et al., 1998). Furthermore, the white muscle in milkfish, which comprises the bulk of the myotomal cones, also deforms in synchrony with local curvature during steady as well as burst swimming (Katz et al., 1999).

Predicting red muscle strain in tuna

The results of the studies mentioned above on other fish led to the expectation that, during steady swimming, red muscle strain would be in phase with local curvature, i.e. that the homogeneous beam model should be appropriate. On the basis of this premise, Knower (1998) measured the patterns of muscle activation in internal red muscle of yellowfin (*Thunnus albacares*) and skipjack (*Katsuwonus pelamis*) tuna during steady swimming, and compared the timing of EMG activity with the phase of muscle strain that was predicted from the local curvature of the body midline. The results were similar in both species but predicted, surprisingly, that red muscle all along the body would be activated only during the latter part of shortening (Fig. 1), a situation that would probably be ineffective in generating positive contractile power and forward thrust. For example, in work-loop studies of fish muscle, maximal positive power output typically occurs when muscle activation begins in the later part of the lengthening phase (Altringham and Johnston, 1990; Johnson and Johnston, 1991; Altringham et al., 1993; Rome and Swank, 1992; Johnston et al., 1993; Hammond et al., 1998). In contrast, the onset of activation during muscle shortening through rest length (as Fig. 1 suggests) results in largely negative work (Johnson and Johnston, 1991; Johnston et al., 1993). In recent *in vitro* experiments with red muscle from yellowfin tuna,

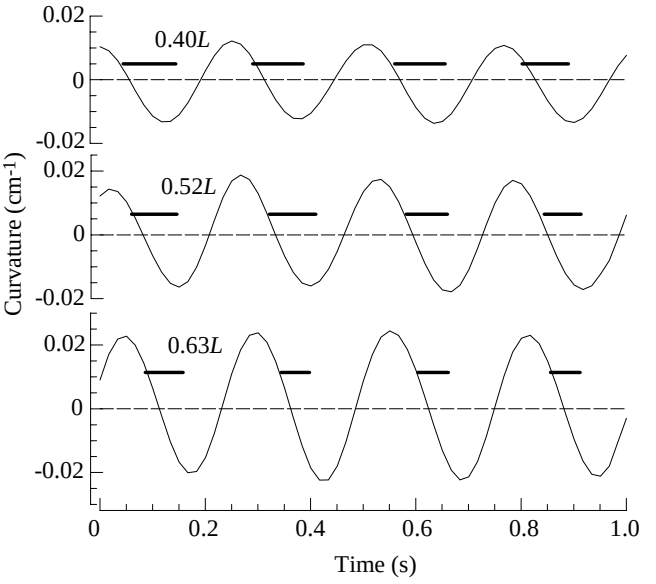

Fig. 1. Comparison of midline curvature (solid lines) and left-side red muscle electromyographic (EMG) activity (horizontal bars) at three locations (0.4*L*, 0.52*L* and 0.63*L*, where *L* is fork length) on a 41 cm skipjack tuna swimming at $2.7\,L\,s^{-1}$. In this scheme, positive curvature indicates that the midline is convex on the left, and negative curvature indicates concavity on the left. On the basis of a simple beam model in which muscle strain coincides with midline curvature, peak muscle length on the left side should occur at maximum curvature, and minimum muscle length should occur at minimum curvature. This model predicts, paradoxically, that muscle activation at all locations does not begin until well after the onset of shortening. Data redrawn from Knower (1998).

Altringham and Block (1997) reported that, as in other fish muscle, the greatest contractile power was produced when the muscle was stimulated whilst lengthening, in this case at approximately 0.13 of a cycle prior to reaching peak length.

These observations yield the following paradox. If tuna muscle is like other fish muscle in the manner in which it generates power, and if red muscle all along the body is activated at a phase that would predict little or no positive power production, then the origin of power for swimming is unknown. But, if muscle activation *in vivo* is coordinated to produce maximum positive power (i.e. activation commencing during late lengthening), then the onset of shortening of the internal red muscle in tunas must occur substantially later than the midline curvature would predict. If this is true, then muscle shortening must be in phase with curvature at more posterior locations, and a simple beam is an inappropriate model of muscle strain in swimming tuna. In the present study, we tested this hypothesis by measuring muscle shortening in swimming skipjack tuna using sonomicrometry and coupling this with muscle activation and midline kinematic data. The results lead to a prediction of how this red muscle functions at different axial locations during swimming.

Materials and methods

Experiments on skipjack tuna (*Katsuwonus pelamis*) were conducted at the National Marine Fisheries Service Kewalo Research Facility in Honolulu, Hawaii, in August 1993 and June 1996. Fish (N=25) ranging in fork length (L) from 0.40 to 0.49 m (1–1.5 kg) were captured on barbless hooks by commercial fishermen and transferred to 7 m diameter (38 000 l) holding tanks with minimal physical handling. The fish were maintained in sea water at 24–26 °C, with continuous flow and aeration, and fed daily *ad libitum* with chopped squid and fish. Experiments were conducted on healthy, feeding fish that had been held for a minimum of 1 week before experiments, and all care and experimental procedures were carried out according to University of California approved protocols.

In vivo *muscle physiology*

Our experiments involved measuring segment length change and electromyographic (EMG) activity within the internal red swimming muscle of fish while they swam at controlled speeds in a 3000 l water tunnel treadmill (described by Dewar and Graham, 1994a). Sonomicrometry is an ultrasonic technique for measuring instantaneous length changes between pairs of piezoelectric crystals implanted in the muscle. The product of the transit time of an ultrasound pulse between the crystals and the speed of sound through muscle (1540 m s^{-1}) is equal to the distance separating the crystals. A sampling rate of 1.25 kHz ensures high temporal resolution, while the ultrasound frequency of 5 MHz yields very short wavelengths and thus high spatial resolution. The use of sonomicrometry in skeletal muscle mechanics of fish has been described previously (Covell et al., 1991; Franklin and Johnston, 1997; Coughlin et al., 1996; Hammond et al., 1998).

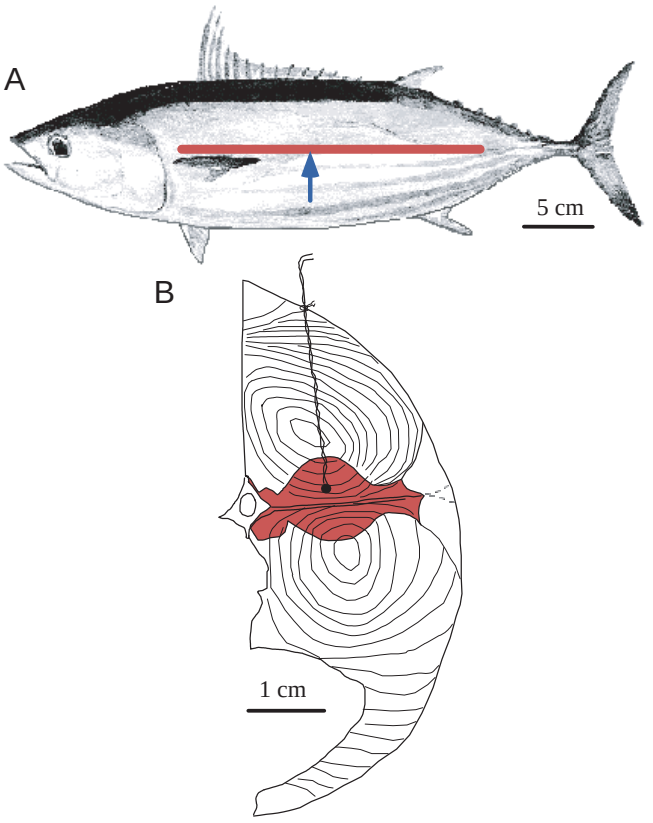

Fig. 2. (A) Lateral view of a skipjack tuna. The red line shows the longitudinal extent of the internalised red muscle. The arrow indicates 0.5L, where L is fork length (adapted from Joseph et al., 1988). (B) View of the left half of a skipkjack tuna, seen in transverse section at 0.5L, illustrating the placement of a sonomicrometer crystal in the internalised red muscle (shaded red). The flexible wire leads are anchored by sutures where they exit the skin, near the dorsal midline. Epaxial (upper) and hypaxial (lower) myotomal cones are represented by the concentric rings.

Surgery was performed under anesthesia to implant sonomicrometer crystals and EMG leads into the internal red muscle mass. Surgical procedures followed those described previously in EMG studies on skipjack and yellowfin tuna (Knower et al., 1999). Briefly, fish were anesthetised quickly by submergence in well-oxygenated sea water containing 1 g l^{-1} MS222 (tricaine methanesulfonate; Finquel, Argent Chemical) buffered to pH 7.8 with Tris base (Sigma Chemical) for 2–3 min. Fish were then transferred to a chamois cradle mounted over the working section of the tunnel and ventilated with a reduced concentration of MS222 (0.057 g l^{-1}) at 23 °C (Korsmeyer et al., 1997). Crystals 2 mm in diameter were constructed from piezoelectric ceramic (LTZ-2 Transducer Products Inc.). After soldering to lead wires, the crystals were lensed with a coating of polyester resin, giving a final thickness of 1.5 mm. Crystal pairs were inserted into the internal red muscle of the left side of the body from near the dorsal midline (Fig. 2). A 2 mm incision was made in the skin, and a puncture was made through the underlying white muscle with a 16 g hypodermic needle, precalibrated to the required depth. This

provided an acceptable probability of placement into the internal red muscle, above the horizontal septum. Correct crystal alignment was ensured by monitoring the RF signal on an oscilloscope (Kirkpatrick et al., 1973). Each pair of crystals was separated along the body axis by 8–15 mm, and three pairs were implanted in each fish at anterior, mid and posterior locations of approximately 0.4*L*, 0.54*L* and 0.7*L*. EMG activity was measured in two ways. In all fish, one bipolar pair of insulated copper wire electrodes (34 gauge, Teflon-coated) with 1 mm bared tips was inserted into the internal red muscle at the anterior crystal site. In addition, EMG activity was recorded at all sonomicrometry sites by demodulating and a.c.-amplifying the signal from the wires of one crystal at each location. This is possible because the EMG signal can be extracted from the kHz range while the ultrasound transit time signal is carried in MHz bands. The validity of the latter measure of EMG timing was confirmed by comparing the two EMG signals available at the anterior location (see example in Fig. 3). The skin holes were closed with a suture, and the wire leads were anchored to the skin in several places next to the dorsal midline. Finally, small pieces of reflective film (4 mm in diameter) were stitched onto the dorsal midline at the leading edge of the first and second dorsal fins (approximately 0.3*L* and 0.6*L*, respectively) to serve as reference landmarks for kinematics analysis (Fig. 4).

The advantages of our surgical approach over a shorter horizontal entry through the superficial red muscle were (1) that the long length of flexible wire between each crystal and the skin (approximately 3 cm) ensured that the crystal would move with the muscle and not be influenced by the skin anchor and (2) that bleeding was minimised. The disadvantage was that crystal implantation was performed somewhat blindly, so our success in obtaining proper alignment and placement within the internal red muscle was not high. *Post-mortem* examination confirmed crystal and EMG electrode placement, and only recordings of strong signals where both crystals were well-situated in red muscle were analysed.

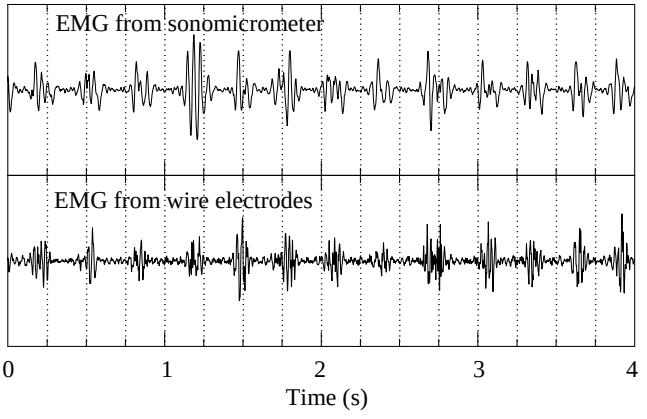

Fig. 3. A comparison of two methods of recording electrical activity in red muscle during steady swimming, showing that the signal from the sonomicrometer crystal wires is a reliable record of electromyographic (EMG) timing and duration. The trace in the top panel was recorded from the sonomicrometer crystal wires, while that in the bottom trace was recorded from bipolar wire EMG electrodes.

After surgery, revival of the fish was initiated by ventilation with clean sea water at 24–26 °C. Recovery was completed in the working section of the water tunnel with water velocity adjusted as the fish regained the ability to swim steadily, a process that generally took 10–30 min. Swimming trials were conducted over the range at which the fish were willing to swim (0.45–1.01 m s^{-1}). EMG signals were conditioned with Grass P15 preamplifiers using a bandwidth of 30–300 Hz. The distance between pairs of sonomicrometer crystals is referred to as muscle 'segment length' and was transduced by a Triton Technology (model 120) sonomicrometer. EMG and length data were recorded digitally on a DOS-based microcomputer at 700 or 1000 Hz per channel, using a TL-2 A/D interface and Axotape software (Axon Instruments Ltd). Simultaneous video images of a dorsal silhouette of the fish against a reflective background (Tang and Wardle, 1992) were collected at 60 Hz (Sony FX-800 8 mm CCD camera, 0.001 s shutter speed). The excitation voltage of a flashing red diode, visible in the video field, was also recorded with the EMG and dimension data for synchronisation purposes.

On the basis of the criteria of high signal-to-noise ratio, correct placement of crystals and steady swimming performance, we selected simultaneous EMG and sonomicrometry data from 12 of 21 possible crystal pairs in 20 swimming bouts (each with a minimum of 10 tail beats) from seven fish. These included four anterior, five mid and three posterior locations. We were unable to obtain successful recordings at all three locations in any one fish. EMG data were filtered and processed digitally as described previously (Knower, 1998; Knower et al., 1999) to determine burst onset and offset times. Muscle segment length signals were low-pass-filtered (see section on kinematics) and corrected for the 5 ms time delay inherent in the output filter of the sonomicrometer. Strain amplitude was calculated as the half-height of the waveform of muscle segment length divided by the mean muscle segment length for that recording.

Kinematics

Kinematic analyses of body bending were performed for nine swimming bouts on five fish, each comprising 4–6 tail beats, following the method of Katz et al. (1999). These recordings were a subset of those used for muscle length analysis. Video images were digitised using a Rasterops video capture board, using MediaGrabber software, on a Macintosh Quadra 700 computer. A 10 cm×10 cm grid on the tunnel floor was used to scale the images, after applying a parallax correction factor calculated by comparing the distance from the snout to the dorsal marker measured in the image with the same distance measured on the fish *post-mortem*. For each video field in a swimming sequence, NIH Image software (http://rsb.info.nih.gov/nih-image/) was used to determine the *x*,*y* coordinates of a series of 20 points along each side of the body outline from approximately the anterior margin of the pectoral fins to the beginning of the peduncle (see Fig. 4). The

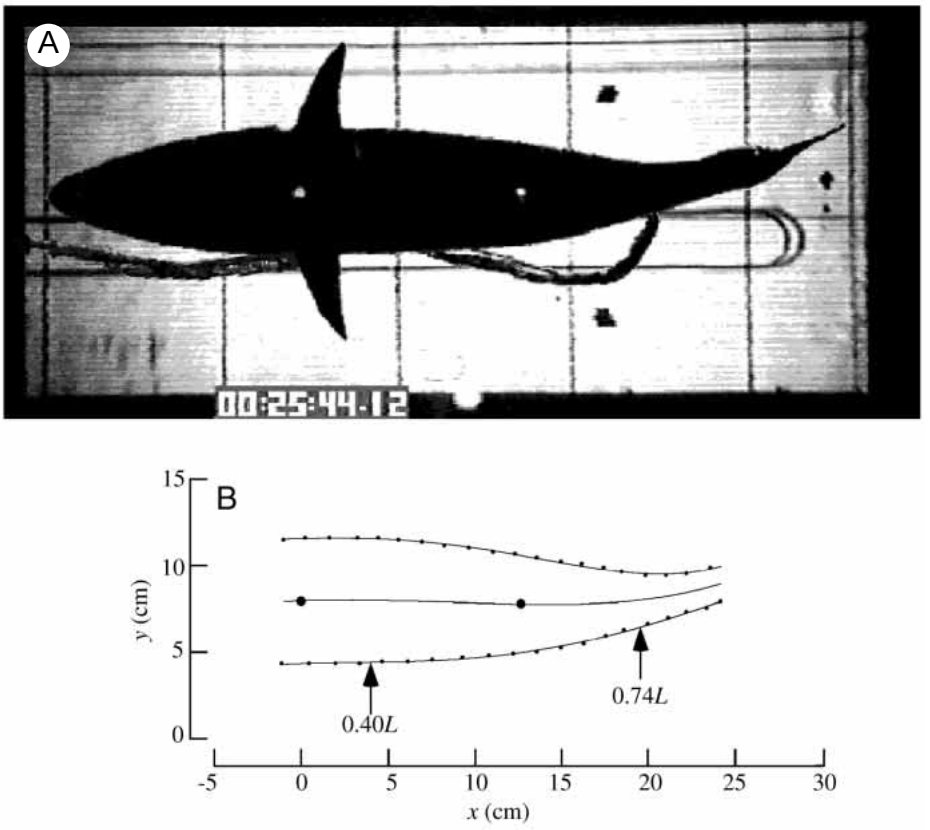

Fig. 4. (A) Example of a video field (1/60 s) of a skipjack swimming in the water tunnel. The fish is silhouetted against a reflective background marked in 10 cm squares. The bundled sonomicrometry lead wires also cast a shadow along the left side of the fish. Anterior and posterior midline reflective markers act as landmarks for kinematic analysis. (B) Polynomial curves fitted to the digitized points along the left and right sides of the silhouette in A and the calculated midline. Note that this curve-fitting procedure was applied to the body only between the anterior margin of the pectoral fin and the beginning of the peduncle, but that these curves extend beyond the region where curvature was calculated (indicated by the arrows at 0.4*L* and 0.74*L*, where *L* is fork length). The *x* coordinate of the anterior dorsal marker is set to zero.

anterior reflective marker was used to align each sequence of images in the rostral–caudal axis, by setting the *x* coordinate of the marker to zero in each field.

Fourth-order polynomial curves were fitted, using a least-squares method, to the points for right and left sides and then averaged to yield fourth-order coefficients that represented the body midline (Fig. 4). These regressions always had r^2>0.98. Since polynomial fits are less reliable near the ends of a data range, we used a series of points on each side that extended well beyond the region (0.4–0.74*L*) where midline curvature was calculated (see Fig. 4). This technique assumes that the midline is not displaced significantly by body thickening on the concave side as the fish bends and, more importantly, that the shape of the midline (i.e. the neutral bending axis) is an average of the shape of the two lateral surfaces. The validity of these assumptions has been demonstrated using X-ray pictures (Rome and Sosnicki, 1991; Wakeling and Johnston, 1998). For our own assessment, we analysed X-ray images of a dead tuna held in a bent configuration similar to the most extreme bending that occurs during swimming. The position of the midline calculated using the above method deviated by no more than 1 mm in the lateral direction from the midline, as defined by the vertebrae, at all locations between the pectoral fins and the peduncle. We also calculated curvature (see below), as a function of axial position, for a line fitted through the centre of the vertebrae in the X-ray image and for the calculated midline; these were in close agreement. For example, the axial location of the peaks in curvature of these two lines matched to within less than 0.5 cm or less than 0.01*L*.

The curvature function, $\kappa(x)$, was calculated for each polynomial function $z(x)$ representing the body midline at a particular time as (Katz and Shadwick, 1998):

$$\kappa(x) = z''(x)/[1 + z'(x)^2]^{3/2},$$

using a custom-designed C+ program for a PowerMacintosh. Note that κ is the inverse of the radius of curvature and that, if κ=0, the line segment is straight. A time series of curvature functions was thus assembled for each swimming sequence and used to determine midline curvature as a function of time at various axial positions corresponding to the locations of the sonomicrometer crystals. The curvature and the muscle segment length signals were then compared after low-pass-filtering with digital finite impulse response filters constructed in AcqKnowledge software (Biopac Systems Inc.) using cut-off frequencies of at least five times the tailbeat frequency for each recording. In our frame of reference, positive curvature indicates that the midline is convex to the left side of the fish, where the sonomicrometry crystals were located. If muscle shortening acts in phase with local midline curvature, then maximum and minimum muscle length would coincide, respectively, with peak positive and peak negative curvature.

Results

Muscle activation and shortening

All observations in this study were made on the internal red muscle used in steady swimming. Typical examples of muscle segment length and EMG activity (Fig. 5) reveal similar patterns

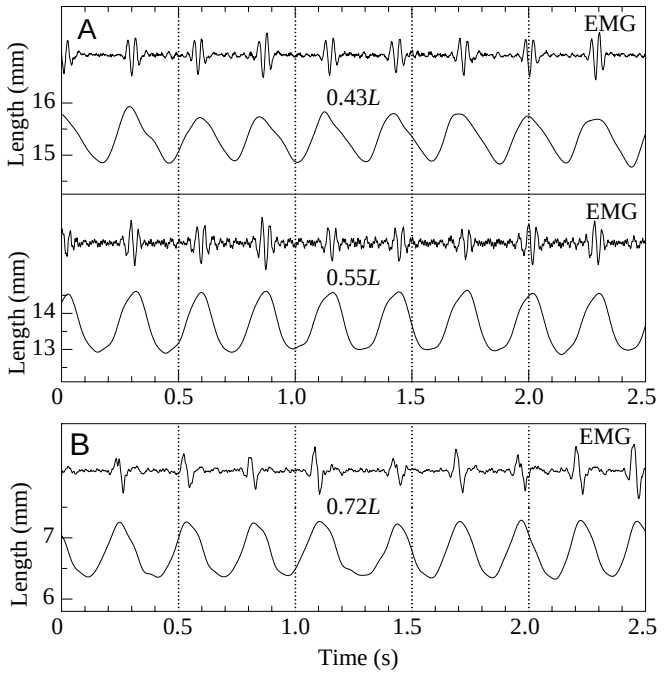

Fig. 5. Examples of muscle electromyographic (EMG) activity and segment length determined using sonomicrometry recorded at three axial locations in two different skipjack tuna. (A) Data from 0.43*L* and 0.55*L* in a 48.6 cm tuna swimming at 1.42 $L\,s^{-1}$, where *L* is fork length. (B) Data from 0.72*L* in a 42.5 cm tuna swimming at 1.74 $L\,s^{-1}$.

of activation at different axial locations. Indeed, at all swimming speeds that we could investigate (1.1–2.3 $L\,s^{-1}$), the onset of muscle activation consistently preceded the onset of muscle shortening at all locations along the body. Furthermore, EMG activity continued well into the period of muscle shortening, with duty cycles of 0.3–0.4 of the tailbeat period. Note that this pattern is quite different from that predicted by assuming that muscle strain is in phase with local curvature (Fig. 1).

Fourier analysis of muscle length change cycles indicated that more than 95 % of the spectral power occurred in the primary harmonic, thus validating a sinusoidal approximation of these events (van Leeuwen et al., 1990; Hess and Videler, 1984; Hammond et al., 1998; Katz et al., 1999). Thus, we adopted the phase scheme suggested by Johnson and Johnston (1991), and followed by others, to describe the relationship between local muscle activation and shortening. Each muscle strain cycle arbitrarily begins (0 °) and ends (360 °) at the point where the muscle length passes through its mean length while lengthening. Consequently, the phase of muscle peak length is 90 °, while the minimum length occurs at 270 °. In this frame of reference, the phases of EMG onsets and offsets are plotted as a function of axial location (Fig. 6), and the data are summarised in Table 1. These results show that, all along the body, EMG onset occurs only during muscle lengthening and EMG offset occurs during shortening. Although the onset of EMG activity in skipjack shows a progressive time delay along the body (Knower et al., 1999), as in other fish (e.g. Wardle et al., 1995; Gillis, 1998), our data show that the phase of EMG onset relative to local muscle shortening changes very little along the body, at least within the range of our measurements (0.40–0.74*L*). While the slope of the regression line for EMG onsets in Fig. 6 is statistically different from zero at $P<0.05$ ($r^2=0.18$; $P=0.048$), the EMG onset phase at 0.69*L* is not significantly earlier than the onset phase at 0.54*L* or 0.41*L* (ANOVA, $F=2.89$, $P=0.08$; see Table 1). Thus, in skipjack tuna, the wave of activation onset appears to travel at approximately the same speed as the wave of muscle contraction, and this results in comparable activation timing of red muscle all along the body. The overall mean activation onset phase was 43.5±9.9 ° (mean ± S.D., $N=22$) for muscle between 0.4*L* and 0.7*L*.

In contrast, red muscle EMG activity in the skipjack ceases nearly simultaneously at all axial locations (Knower et al., 1999), reflecting the caudally decreasing EMG duty cycle

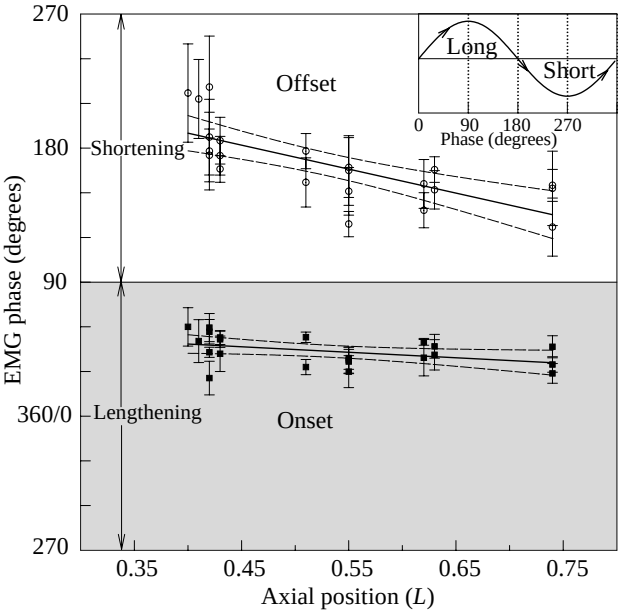

Fig. 6. A summary diagram of the phase of activation relative to the local strain cycle of internal red muscle at different positions along the body for swimming speeds of 1.1–2.3 $L\,s^{-1}$, where *L* is fork length. The vertical axis represents one cycle of muscle strain (as indicated by the sinusoid in the inset) that arbitrarily begins (0 °) at mean length while lengthening (Johnson and Johnston, 1991). Thus, peak length occurs at a phase of 90 °, minimum length at 270 ° and mean length while shortening at 180 °. The shaded area represents the lengthening portion of the muscle strain cycle (270–90 °), while the unshaded area represents muscle shortening (90–270 °). Both electromyographic (EMG) onset (filled squares; means ± S.D. $N=22$) and offset (open circles; means ± S.D., $N=22$) data are plotted along with fitted linear regressions and their 95 % confidence intervals. The EMG onset regression is described by the equation: $\phi=63.1-36.8L$ (where ϕ is phase; $r^2=0.18$, $F=4.44$, d.f.=1,20, $P=0.048$), indicating that the phase of muscle activation is nearly the same at all positions along the body and occurs prior to peak muscle length. In contrast, the EMG offsets occur during shortening but at a relatively earlier phase in the more posterior locations. These data are described by the equation: $\phi=254.4-160.8L$ ($r^2=0.54$, $F=23.3$, d.f.=1,20, $P<0.001$).

Table 1. *Mean peak muscle strain amplitude and activation phase in skipjack tuna swimming at speeds of 1.1 to 2.3* L s^{-1}

Position	*L*	±Strain	EMG on (degrees)	EMG off (degrees)
Anterior	0.41±0.01	0.054±0.016	49.0±10.9	190.8±19.8
Mid	0.54±0.02	0.066±0.018	38.2±8.0^{NS}	157.8±16.8*
Posterior	0.69±0.06	0.082±0.027	41.0±7.5^{NS}	149.6±12.8*

Phase is expressed relative to muscle strain at each location, as in Fig. 6.
Values are means ± S.D., *N*=9 (anterior), 6 (mid), 7 (posterior).
*Indicates a significant difference in electromyogram (EMG) phase from the value at the anterior position at $P<0.01$.
^{NS}Indicates no significant difference from the phase at the anterior position at $P>0.05$.
L, fork length.

(Fig. 6; Table 1). Consequently, the phase of EMG cessation, relative to the travelling wave of muscle contraction, is earlier in more posterior locations, i.e. the slope of the EMG offset line in Fig. 6 is significant (r^2=0.54; $P<0.001$); EMG offset occurred at approximately 191 ° at 0.41*L* and at approximately 150 ° at 0.69*L* (Table 1). The phase relationships between red muscle activation and shortening at each axial location were independent of swimming speed (data not shown).

Table 1 also shows that the mean strain amplitude of the internal red muscle monitored in this study ranged from approximately 0.054 anteriorly to 0.082 posteriorly, at swimming speeds of 1.1–2.3 *L* s^{-1}. No significant correlation between muscle strain amplitude and swimming speed was found for any axial position. This is consistent with our observation that increases in swimming speed resulted from increases in tailbeat frequency alone, as has been demonstrated previously for tunas (Dewar and Graham, 1994b; Knower, 1998; Knower et al., 1999) and other fish (Hunter and Zweifel, 1971; Webb et al., 1984; Lowe, 1996; Katz et al., 1999).

Muscle shortening versus *local curvature*

Our analysis of midline curvature as a function of time revealed that, at axial locations between 0.4*L* and 0.74*L*, muscle strain is not in phase with local body curvature. Fig. 7 gives examples of this result at 0.41*L* and 0.63*L*, respectively. In each case, the maximum in local curvature (i.e. the greatest convexity to the left) precedes the peak in muscle length on the left side by approximately 0.15 cycles. In fact, by the time muscle shortening begins at each site, local curvature is approaching zero (i.e. straight). Consequently, changes in muscle length along this region are in phase with changes in curvature at locations several centimeters more posterior. For example, muscle strains at 0.41*L* and 0.63*L* are approximately in phase with local curvature at 0.56*L* and 0.82*L* (or +6.5 and +8 cm more posterior), respectively. Fig. 8 summarises the results for five fish, showing that the phase lag of muscle strain relative to local curvature is independent of position along the body. The mean phase lag was 48.3±12.6 ° (mean ± S.D.). These data suggest that the waves of muscle contraction and body curvature travel at comparable rates along the fish, although the peak strains are always later than the peaks in curvature. Again, no effect of swimming speed was evident on this phase relationship.

Muscle shortening versus *tail deflection*

Our general finding was that the minimum in muscle length at sites along the left side of the body corresponded closely to the time at which the tip of the caudal fin reached its greatest

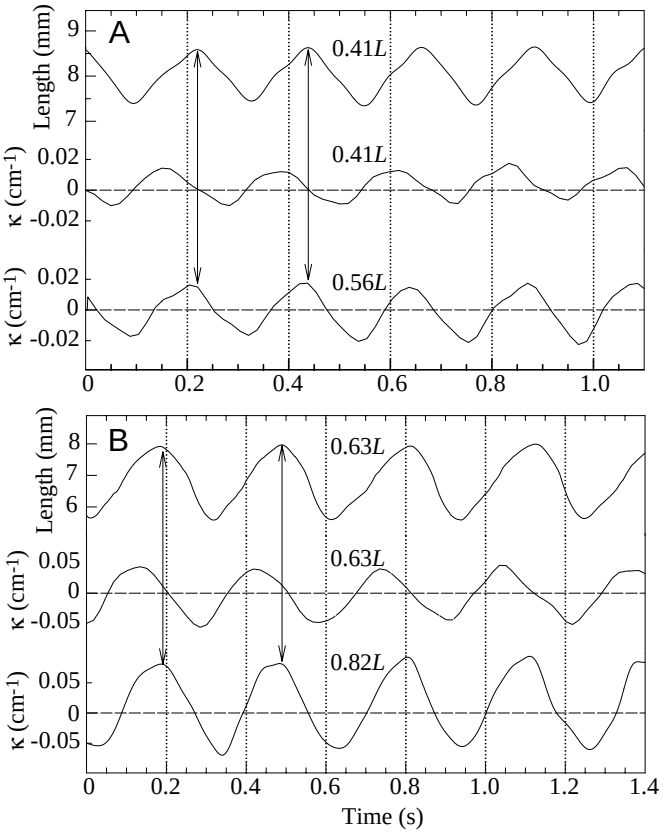

Fig. 7. (A) Muscle segment length on the left side of the body at 0.41*L*, where *L* is fork length, in a 43.5 cm skipjack swimming at 2.1 *L* s^{-1} compared with midline curvature (κ) at that same location and at a more posterior location of 0.56*L*. (B) Muscle segment length on the left side of the body at 0.63*L* in a 42.5 cm skipjack swimming at 1.75 *L* s^{-1} compared with κ at 0.63*L* and 0.82*L*. As defined by equation 1, $\kappa>0$ indicates that the midline is convex on the left, $\kappa<0$ indicates that the midline is concave on the left, and $\kappa=0$ indicates that the midline is straight. Inspection of these data show that muscle strain is phase-delayed relative to local curvature and that the peak in muscle length coincides with the peak in convex curvature at locations that are 6.5–8 cm more posterior (arrows).

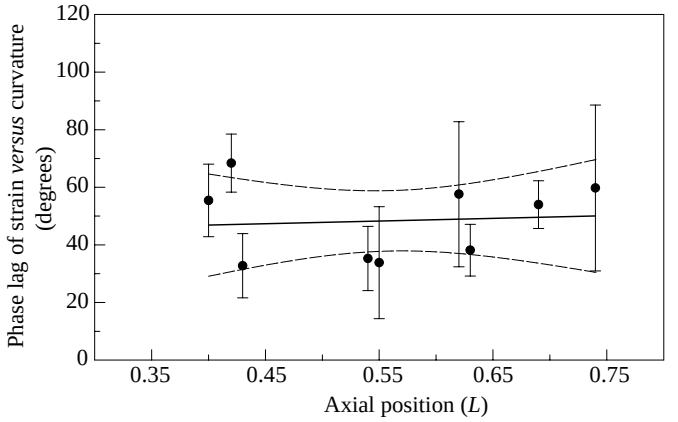

Fig. 8. The phase lag of red muscle shortening relative to local midline curvature for axial locations of 0.4*L* to 0.74*L*, where *L* is fork length. Values are means ± S.D. for sequences of five tail beats for each of nine swimming bouts in five fish at speeds of 1.08–2.25 $L\,s^{-1}$. A linear regression of the data (solid line) and 95 % confidence limits (dashed lines) are shown. The slope of this line is not significantly different from zero (r^2=0.007, P=0.82), and the overall mean phase lag is 48.3±12.6 °.

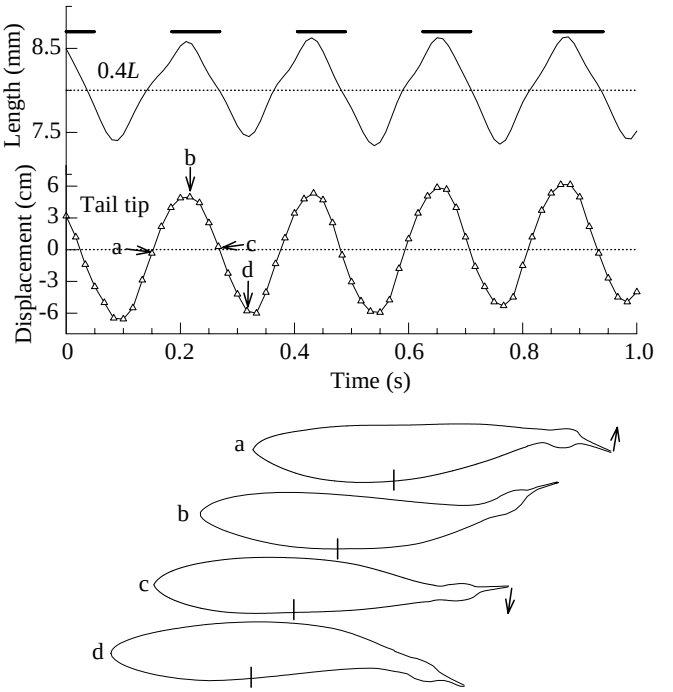

Fig. 9. A plot of the muscle strain cycle on the left side at 0.4*L* (upper trace) compared with the lateral excursion of the tail tip (lower trace) in a 43.5 cm skipjack swimming at 2.1 $L\,s^{-1}$, where *L* is fork length. Horizontal bars in the top panel indicate the timing of electromyographic (EMG) activity in successive tail beats for that axial location. In our kinematic frame of reference, tail tip displacement towards the right side of the fish is indicated by positive values. The four body outlines below coincide with the points labelled a, b, c and d on the displacement trace. The vertical bars on each outline indicate the location of the muscle length measurement (0.4*L*). These data demonstrate that the time of minimum muscle length on the left coincides with maximum tail tip deflection to that side, while peak muscle length on the left occurs as the tail tip reaches the extreme deflection on the right side. The arrows indicate the direction of movement of the tail tip.

lateral deflection to that side. At 0.4*L*, muscle shortening and tail tip displacement are virtually in phase, i.e. muscle shortening on the left side begins when the tail tip is at its right-most position (point b, Fig. 9) and ends when the tail tip is at its left-most position (point d, Fig. 9). The strain peaks are only slightly later at 0.7*L*, because the wave of muscle strain travels very rapidly. Although we did not measure the speed at which the onset of muscle shortening travels along the body, it can be estimated from the phase data in Table 1. Because the cessation of EMG activity is virtually simultaneous in absolute time between 0.4*L* and 0.7*L* (Knower et al., 1999), the difference in phase of EMG offset relative to muscle strain is a measure of the progression of strain peaks along the body. Table 1 shows this phase difference to be approximately 41 ° (=0.11 cycle) over a distance of 0.28*L*, yielding a muscle strain wave speed of 2.5*L* per cycle period, at least through the region where most of the red muscle resides. Because shortening onset at anterior and posterior sites differs by only approximately 10 % of a tailbeat cycle, this means that the muscle all along that side is in its shortening phase for 80 % of the time during which the tail tip is travelling to one side.

Discussion

Many anatomical and physiological features of tunas point towards a design for high-performance swimming. Among these, the great elongation of myotomes and their posterior projections to the skin and axial skeleton by myosepta and tendons suggest that the action of the swimming muscle is directed back to the thrust-producing caudal fin (Fierstine and Walters, 1968). In the present study, we present evidence to support this view: the internal red muscle of skipjack tuna, while primarily located in mid-body regions, functions as a forceful actuator that delivers contractile power to posterior locations on the body. Although muscle activation and the onset of shortening proceed along the body in time, the transmission of these events is so rapid that muscle contraction is nearly synchronous along each entire side of the body. This, coupled with the caudally directed action of the contracting muscle, yields the features that are the hallmark of ‘thunniform’ locomotion, namely a low-amplitude body wave and powerful lateral undulations of the thrust-producing lunate caudal fin (Fierstine and Walters, 1968; Magnuson, 1978). We anticipate that these general conclusions also apply to yellowfin tuna because of the similarities in anatomy and in the phase relationship between curvature and activation reported by Knower (1998).

To quantify work and power output with certainty, direct measurements of instantaneous muscle force and shortening *in vivo* are needed. While muscle shortening can be measured using sonomicrometry, the anatomical peculiarities of fish

myotomes render direct force measurement from specific muscles very difficult, and this has not been accomplished in any fish. Instead, muscle performance is predicted on the basis of *in vitro* cyclic work-loop experiments that use activation and strain parameters gathered from *in vivo* measurements. In all studies of fish locomotor muscle reported to date, maximal positive contractile work is achieved in cyclic contractions when muscle stimulation precedes the peak length by approximately 0.06–0.20 of a cycle period (depending on strain amplitude, frequency and temperature), i.e. at activation phases of 20–70 °, as defined in Fig. 6 (see, for example, Altringham and Johnston, 1990; Johnson and Johnston, 1991; Johnson et al., 1994; Rome et al., 1993; Hammond et al., 1998). This behaviour is typical of vertebrate skeletal muscle and reflects the contractile properties of the sliding filament system. Pre-stretch of activated muscle and strain-dependent shortening-enhanced relaxation are important contributors to maximising power production. Activation during the final portion of the lengthening phase allows the muscle to develop higher than isometric force during a short period of negative (energy-absorbing) work, to maintain high force during the shortening phase and to be inactive during lengthening (van Leeuwen, 1995). Experimentally, these conditions yield large net-positive power during cyclic contractions.

Muscle activation and function in skipjack tuna

The present study demonstrates that the onset of activation of the internal red muscle in the skipjack tuna occurs at virtually the same phase relative to local shortening at axial locations between approximately 0.4*L* and 0.74*L*, where the bulk of red muscle is found (Graham et al., 1983). Furthermore, EMG activity always begins during muscle lengthening, at a phase of 40–50 °, indicating that force enhancement by stretching probably occurs in all red muscle. Note that these results are substantially different from what was predicted from curvature in Fig. 1 (see below). On the basis of the above discussion, this activation timing should result in similar muscle function and net-positive work output at all axial locations. Furthermore, these activation phases are very close to those producing maximum power in work-loop studies of red muscle from yellowfin tuna (Altringham and Block, 1997). Specifically, Altringham and Block (1997) reported that optimal stimulation phase increased from 20 to 60 ° as muscle temperature was varied from 15 to 30 °C. With the ambient water temperature of 24–26 °C in the present study, *in vivo* red muscle temperature was probably in the range 27–29 °C (Dizon and Brill, 1979). Assuming comparable contractile properties in skipjack and yellowfin red muscle, and interpolating the results of Altringham and Block (1997), we can predict optimal activation phase of red muscle for our experiments to be 52–57 °, very close to the range we measured. Thus, it seems likely that all the internal red muscle is functioning to produce maximal positive power during steady swimming. Furthermore, the modest increase in strain amplitude caudally and the relatively constant cross section of red muscle, at least between 0.4 and 0.6*L* (Graham et al., 1983; Knower, 1998), suggest that the absolute work per cycle (and power output) may be fairly uniform along most of the body. We acknowledge, however, that these conclusions await confirmation by *in vitro* work-loop tests of muscle from different axial sites in skipjack tuna. In particular, it will be important to elucidate to what extent, if any, the contractile properties of this muscle vary along the body, as appears to be the case in bluefin and yellowfin tuna (Wardle et al., 1989; Altringham and Block, 1997). It must also be determined how decreased duty cycles in posterior locations influence muscle performance *in vitro* and *in vivo*.

Our results are substantially different from models of axial muscle function for swimming in other fish (Hess and Videler, 1984; van Leeuwen et al., 1990; Altringham et al., 1993; Wardle and Videler, 1994; Hammond et al., 1998). In particular, our observation that waves of muscle shortening and EMG activity onset travel along the body at nearly equal rates, so that muscle at all axial locations is activated at essentially the same strain phase, has not been reported previously in other species. Instead, there is an increasing phase advance of the activation onset relative to muscle shortening in all other fish studied to date, because these events progress along the body at different speeds (summarised by Gillis, 1998). This anterior–posterior phase shift ranges from approximately $180\,^{\circ}\,L^{-1}$ in the bass *Micropterus salmoides* to approximately $65\,^{\circ}\,L^{-1}$ in the scup *Stenotomus chrysops*. Recent work by Hammond et al. (1998) has demonstrated an anterior–posterior phase shift in muscle activation of approximately $95\,^{\circ}\,L^{-1}$ in the rainbow trout *Oncorhynchus mykiss*. While variation in activation phase advance may be associated with differences in myotome structure, the specific details of this relationship have not yet been resolved.

Wardle et al. (1995) proposed that fish such as a mackerel, that swim by producing thrust mostly at the tail fin, should have the greatest EMG phase advance caudally, so that posterior muscle will be actively stretched while anterior muscle contracts to produce positive power. In this model, the primary role of the posterior myotomes is to perform negative work and to act as stiff transmitters of power from the anterior myotomes to the tail fin. An alternative view, based on studies of the scup, is that posterior muscle generates the majority of positive power for thrust, while anterior muscle contributes relatively little (Rome et al., 1993; Coughlin and Rome, 1996). We suggest that the role of power production in skipjack tuna is probably distributed uniformly along the body, with force transmission being provided primarily by connective tissue structures rather than by muscles performing negative work. These structures include the skin, oblique tendons in the horizontal septum and robust caudal tendons (Kishinouye, 1923; Kafuku, 1954; Fierstine and Walters, 1968; Westneat et al., 1993).

If we consider tunas as high-performance swimmers, our view of their red muscle function seems more compelling than the models of either the Wardle or Rome groups for two reasons. First, all the red muscle mass would contribute substantial positive power, thus maximising the total mass-specific power. Second, the use of stiff and resilient

collagenous tissues such as tendons (Shadwick et al., 1992; Knower, 1998) to transmit force is much more energetically efficient than the use of actively stretched muscle (Alexander and Bennet-Clark, 1977). It is important to remember that, in a swimming fish, muscle performing negative work is absorbing energy produced by some other source, probably another muscle. So, while an active muscle that is stretched may produce higher forces than during shortening, it is not adding to the thrust force at the tail.

Muscle shortening versus *local curvature*

In addition to their unique muscle activation and strain pattern, a critical distinction between skipjack tuna and other fish is the apparent uncoupling of red muscle strain from local body bending. Unlike contraction of the superficial red muscle in other fish, the shortening of internal red muscle in skipjack tuna lags significantly behind changes in the local midline curvature (Fig. 8). Thus, at sites between 0.4*L* and 0.74*L*, peak muscle length occurs after the maximum convex curvature to that side and, likewise, minimum muscle length occurs after the greatest concave curvature. This observation explains the paradoxical activation timing presented in Fig. 1, which resulted from assuming that strain was in phase with curvature. In skipjack tuna, the temporal separation of red muscle strain and local curvature is so pronounced that, in the mid-body region, muscle shortening at each location is synchronous with midline curvature at locations that are 7–8 cm (or 8–10 vertebral segments) more posterior (Fig. 7). Interestingly, this distance closely matches the span of the elongated myotomes in skipjack tuna (Fierstine and Walters, 1968). Our results suggest that contraction of the internal red muscle causes deformation of the body at more posterior locations, rather than locally. This situation represents a unique departure from the model of a homogeneous bending beam, which describes red muscle strain in other fish during steady swimming, but is consistent with the premise that tunas produce thrust by motion of the caudal fin rather than by undulation of segments along the body (Fierstine and Walters, 1968; Lighthill, 1970).

How could muscle shortening be uncoupled from local bending? Wainwright (1983) and Westneat et al. (1993) proposed that fish myotomal cones transmit their contractile force caudally along the backbone *via* myoseptal and dermal connective tissue linkages. In tunas, the contraction of red muscle could project caudally *via* the posterior oblique tendons that lie within the horizontal septum, the myoseptal connections to the skin and, at the most posterior sites, the robust tendons that link directly onto the caudal fin rays (Fierstine and Walters, 1968). In this manner, the local shortening could cause bending at more posterior locations.

If our conclusions are correct, then shearing must occur between the internal loin of red muscle and the surrounding mass of white muscle which, while inactive, is surely strained in synchrony with the bending midline. How this may change when the white muscle actively shortens in fast swimming is not yet known. In maximal myotomal contractions powering fast starts of rainbow trout, Covell et al. (1991) found that white muscle shortening was not in phase with local curvature, and they concluded that myotomal deformation was coupled to more posterior locations by skeletal or other structures. In contrast, white muscle used in burst swimming by milkfish and in fast starts by carp (*Cyprinus carpio*) shortened in phase with superficial red muscle and in phase with local midline curvature (Katz et al., 1999; Wakeling and Johnston, 1999), as predicted by a simple beam model. Interestingly, tunas also have some superficially located red muscle which, if coupled to the overlying skin, might contract in phase with local curvature and, therefore, also shear relative to the adjacent internal red muscle. Future studies should resolve such issues and shed further light on the mechanical consequences of the internal positioning of red muscle in tunas.

The authors thank Drs Richard Brill, Kathy Cousins, Tim Lowe and Michael Laurs for their generous hospitality and assistance at the Kewalo Basin Research Facility and Jeffrey Graham for help in developing the water tunnel techniques. Dr Bradley Shadwick kindly wrote the computer program for curvature analysis and Dr Lewis Waldman gave helpful advice on image processing. We also thank Drs J. D. Altringham, G. Biersch, L. Hammond, U. Müller, C. S. Wardle and J. J. Videler for enjoyable and stimulating discussion at various points in the development of this material. This research was supported by the National Science Foundation (OCE91-03739 and IBN95-14203).

References

Alexander, R. McN. and Bennet-Clark, H. C. (1977). Storage of elastic strain energy in muscle and other tissues. *Nature* **265**, 114–117.

Altringham, J. D. and Block, B. A. (1997). Why do tuna maintain elevated slow muscle temperatures? Power output of muscle isolated from endothermic and ectothermic fish. *J. Exp. Biol.* **200**, 2617–2627.

Altringham, J. D. and Johnston, I. A. (1990). Modelling muscle power output in a swimming fish. *J. Exp. Biol.* **148**, 395–402.

Altringham, J. D., Wardle, C. S. and Smith, C. I. (1993). Myotomal muscle function at different locations in the body of a swimming fish. *J. Exp. Biol.* **182**, 191–206.

Bone, Q. (1978). Locomotor muscle. In *Fish Physiology*, vol. VII (ed. W. S. Hoar and D. J. Randall), pp. 361–424. New York: Academic Press.

Brill, R. W. (1996). Selective advantages conferred by the high performance physiology of tunas, billfishes and dolphin fish. *Comp. Biochem. Physiol.* **113**A, 3–15.

Brill, R. W. and Dizon, A. E. (1979). Red and white muscle fibre activity in swimming skipjack tuna, *Katsuwonus pelamis* (L.). *J. Fish Biol.* **15**, 679–685.

Cheng, J.-Y., Pedley, T. J. and Altringham, J. D. (1998). A continuous dynamic beam model for swimming fish. *Phil. Trans. R. Soc. Lond. B* **353**, 981–997.

Coughlin, D. J. and Rome, L. C. (1996). The roles of pink and red muscle in powering steady swimming in scup, *Stenotomus chrysops*. *Am. Zool.* **36**, 666–677.

Coughlin, D. J., Valdes, L. and Rome, L. C. (1996). Muscle length

changes during swimming in scup: sonomicrometry verifies the anatomical high-speed cine technique. *J. Exp. Biol.* **199**, 459–463.

Covell, J. W., Smith, M., Harper, D. G. and Blake, R. W. (1991). Skeletal muscle deformation in the lateral muscle of the intact rainbow trout *Oncorhynchus mykiss* during fast start maneuvers. *J. Exp. Biol.* **156**, 453–466.

Dewar, H. and Graham, J. B. (1994a). Studies of tropical tuna swimming performance in a large water tunnel. I. Energetics. *J. Exp. Biol.* **192**, 13–31.

Dewar, H. and Graham, J. B. (1994b). Studies of tropical tuna swimming performance in a large water tunnel. III. Kinematics. *J. Exp. Biol.* **192**, 45–59.

Dizon, A. E. and Brill, R. W. (1979). Thermoregulation in tunas. *Am. Zool.* **19**, 249–265.

Fierstine, H. L. and Walters, V. (1968). Studies in locomotion and anatomy of scombroid fishes. *Mem. S. Calif. Acad. Sci.* **6**, 1–31.

Franklin, C. E. and Johnston, I. A. (1997). Muscle power output during escape responses in an Antarctic fish. *J. Exp. Biol.* **200**, 703–712.

Gillis, G. B. (1998). Neuromuscular control of anguilliform locomotion: patterns of red and white muscle activity during swimming in the American eel *Aguilla rostrata*. *J. Exp. Biol.* **201**, 3245–3256.

Graham, J. B., Koehrn, F. J. and Dickson, K. A. (1983). Distribution and relative proportions of red muscle in scombrid fishes: consequences of body size and relationships to locomotion and endothermy. *Can. J. Zool.* **61**, 2087–2096.

Hammond, L., Altringham, J. D. and Wardle, C. S. (1998). Myotomal slow muscle function of rainbow trout *Oncorhynchus mykiss* during steady swimming. *J. Exp. Biol.* **201**, 1659–1671.

Hess, F. and Videler, J. J. (1984). Fast continuous swimming of saithe (*Pollachius virens*): a dynamic analysis of bending movements and muscle power. *J. Exp. Biol.* **109**, 229–251.

Hunter, J. R. and Zweifel, J. R. (1971). Swimming speed, tail beat frequency, tail beat amplitude and size in jack mackerel, *Trachurus symmetricus* and other fishes. *Fish. Bull. Fish Wildl. Serv. US* **69**, 253–266.

Jayne, B. C. and Lauder, G. V. (1995). Speed effects on midline kinematics during steady undulatory swimming of largemouth bass *Micropterus salmoides*. *J. Exp. Biol.* **198**, 585–602.

Johnson, T. P. and Johnston, I. A. (1991). Power output of fish muscle fibres performing oscillatory work: effects of acute and seasonal temperature change. *J. Exp. Biol.* **157**, 409–423.

Johnson, T. P., Syme, D. A., Jayne, B. C. and Lauder, G. V. (1994). Modeling red muscle power output during steady and unsteady swimming in largemouth bass. *Am. J. Physiol.* **36**, R481–R488.

Johnston, I. A., Franklin, C. E. and Johnson, T. P. (1993). Recruitment patterns and contractile properties of fast muscle fibres isolated from rostral and caudal myotomes of the short-horned sculpin. *J. Exp. Biol.* **185**, 251–265.

Joseph, J., Klawe, W. and Murphy, P. (1988). *Tuna and Billfish. Fish Without a Country*. La Jolla, CA: Inter-American Tropical Tuna Commission.

Kafuku, T. (1950). Red muscles in fishes. I. Comparative anatomy of the scombroid fishes of Japan. *Jap. J. Ichthyol.* **1**, 89–100.

Katz, S. L. and Shadwick, R. E. (1998). Curvature of swimming fish midlines as an index of muscle strain suggests swimming muscle produces net positive work. *J. Theor. Biol.* **193**, 243–256.

Katz, S. L., Shadwick, R. E. and Rapoport, H. S. (1999). Muscle strain histories in swimming milkfish in steady and sprinting gaits. *J. Exp. Biol.* **202**, 529–541.

Kirkpatrick, S. W., Covell, J. W. and Friedman, W. F. (1973). A new technique for the continuous assessment of fetal and neonatal cardiac performance. *Am. J. Obstet. Gynec.* **116**, 963–972.

Kishinouye, K. (1923). Contributions to the comparative study of the so-called scombroid fishes. *J. Coll. Agric Imper. Univ. Tokyo* **8**, 293–475.

Knower, T. (1998). Biomechanics of thunniform swimming. PhD thesis, University of California, San Diego.

Knower, T., Shadwick, R. E., Katz, S. L., Graham, J. B. and Wardle, C. S. (1999). Red muscle activation patterns in yellowfin (*Thunnus albacares*) and skipjack (*Katsuwonas pelamis*) tunas during steady swimming. *J. Exp. Biol.* **202**, 2127–2138.

Korsmeyer, K. E., Lai, N. C., Shadwick, R. E. and Graham, J. B. (1997). Heart rate and stroke volume contributions to cardiac output in swimming yellowfin tuna: response to exercise and temperature. *J. Exp. Biol.* **200**, 1975–1986.

Lighthill, M. J. (1970). Aquatic animal propulsion of high hydromechanical efficiency. *J. Fluid Mech.* **44**, 265–301.

Long, J. H., Jr (1998). Muscles, elastic energy and the dynamics of body stiffness in swimming eels. *Am. Zool.* **38**, 771–792.

Long, J. H., Jr and Nipper, K. S. (1996). The importance of body stiffness in undulatory propulsion. *Am. Zool.* **36**, 678–694.

Lowe, C. G. (1996). Kinematics and critical swimming speed of juvenile scalloped hammerhead sharks. *J. Exp. Biol.* **199**, 2605–2610.

Magnuson, J. J. (1978). Locomotion in scombrid fishes: hydrodynamics, morphology, and behavior. In *Fish Physiology. Locomotion*, vol. VII (ed. W. S. Hoar and D. J. Randall), pp. 239–313. New York: Academic Press.

Rayner, M. D. and Keenan, M. J. (1967). Role of red and white muscles in the swimming of skipjack tuna. *Nature* **214**, 392–393.

Rome, L. C. and Sosnicki, A. A. (1991). Myofilament overlap in swimming carp. II. Sarcomere length changes during swimming. *Am. J. Physiol.* **260**, C289–C296.

Rome, L. C. and Swank, D. (1992). The influence of temperature on power output of scup red muscle during cyclic length changes. *J. Exp. Biol.* **171**, 261–282.

Rome, L. C., Swank, D. and Corda, D. (1993). How fish power swimming. *Science* **261**, 340–343.

Shadwick, R. E., Knower, T. and Fonseca, M. (1992). The mechanical organization of muscle and tendon in yellowfin tuna. *Am. Zool.* **32**, 159A.

Shadwick, R. E., Steffensen, J. F., Katz, S. L. and Knower, T. (1998). Muscle dynamics in fish during steady swimming. *Am. Zool.* **38**, 755–770.

Tang, J. and Wardle, C. S. (1992). Power output of two sizes of Atlantic salmon (*Salmo salar*) at their maximum sustained swimming speeds. *J. Exp. Biol.* **166**, 33–46.

van Leeuwen, J. L. (1995). The action of muscles in swimming fish. *Exp. Physiol.* **80**, 177–191.

van Leeuwen, J. L., Lankheet, M. J. M., Akster, H. A. and Osse, J. W. M. (1990). Function of red axial muscles of carp (*Cyprinus carpio*): recruitment and normalized power output during swimming in different modes. *J. Zool., Lond.* **220**, 123–145.

Videler, J. J. (1993). *Fish Swimming*. London: Chapman & Hall.

Wainwright, S. A. (1983). To bend a fish. In *Fish Biomechanics* (ed. P. W. Webb and D. Weihs), pp. 68–91. New York: Praeger Publ.

Wakeling, J. M. and Johnston, I. A. (1998). Muscle power output limits fast-start performance in fish. *J. Exp. Biol.* **201**, 1505–1526.

Wakeling, J. M. and Johnston, I. A. (1999). White muscle strain in

the common carp and red to white muscle gearing ratios in fish. *J. Exp. Biol.* **202**, 521–528.

Wardle, C. S. and Videler, J. J. (1993). The timing of the electromyogram in the lateral myotomes of mackerel and saithe at different swimming speeds. *J. Fish Biol.* **42**, 347–359.

Wardle, C. S. and Videler, J. J. (1994). The timing of lateral muscle strain and EMG activity in different species of steadily swimming fish. In *Mechanics and Physiology of Animal Swimming* (ed. L. Maddock, Q. Bone and J. M. V. Rayner), pp. 111–118. Cambridge: Cambridge University Press.

Wardle, C. S., Videler, J. J. and Altringham, J. D. (1995). Tuning in to fish swimming waves: body form, swimming mode and muscle function. *J. Exp. Biol.* **198**, 1629–1636.

Wardle, C. S., Videler, J. J., Arimoto, T., Franco, J. M. and He, P. (1989). The muscle twitch and the maximum swimming speed of giant bluefin tuna, *Thunnus thynnus* L. *J. Fish Biol.* **35**, 129–137.

Webb, P. W., Kostecki, P. T. and Stevens, E. D. (1984). The effect of size and swimming speed on locomotor kinematics of rainbow trout. *J. Exp. Biol.* **109**, 77–95.

Westneat, M. W., Hoese, W., Pell, C. A. and Wainwright, S. A. (1993). The horizontal septum mechanisms of force transfer in locomotion of scombrid fishes Scombridae Perciformes. *J. Morph.* **217**, 183–204.

Williams, T. L., Grillner, S., Smoljaninov, V. V., Wallen, P., Kashin, S. and Rossignol, S. (1989). Locomotion in lamprey and trout: the relative timing of activation and movement. *J. Exp. Biol.* **143**, 559–566.